Pis'ma v ZhETF, vol. 94, iss. 6, pp. 513 – 516

Digital photocontrol of the network of live excitable cells

I. S. Erofeev[+], N. Magome[○], K. I. Agladze[+○1)]

[+]Research and Education Center Bionanophysics, Moscow Institute of Physics and Technology
141700 Dolgoprudny, Russia

[○]Institute for Integrated Cell-Material Sciences, Kyoto University, 606-8501 Kyoto, Japan

Submitted 3 August 2011

Recent development of tissue engineering techniques allows creating and maintaining almost indefinitely networks of excitable cells with desired architecture. We coupled the network of live excitable cardiac cells with a common computer by sensitizing them to light, projecting a light pattern on the layer of cells, and monitoring excitation with the aid of fluorescent probes (optical mapping). As a sensitizing substance we used azobenzene trimethylammonium bromide (AzoTAB). This substance undergoes *cis-trans*-photoisomerisation and *trans*-isomer of AzoTAB inhibits excitation in the cardiac cells, while *cis*-isomer does not. AzoTAB-mediated sensitization allows, thus, reversible and dynamic control of the excitation waves through the entire cardiomyocyte network either uniformly, or in a preferred spatial pattern. Technically, it was achieved by coupling a common digital projector with a macroview microscope and using computer graphic software for creating the projected pattern of conducting pathways. This approach allows real time interactive photocontrol of the heart tissue.

1. Introduction. Excitable networks of various origins, such as networks of neural cells, oscillating chemical media, solid state chips exhibiting self-sustained waves (autowaves), etc. always teased computer scientists as possible prototypes for highly parallel computer processors [1–8]. From the other hand, recent development of tissue engineering techniques allows to create and maintain almost indefinitely networks of excitable cells with desired architecture [9–11]. One challenging aspect of such systems is creating an interface allowing coupling the network of live excitable cells with a common computer. We are approaching this goal by sensitizing excitable cardiac cells to light and monitoring excitation in them with the aid of fluorescent probes (optical mapping). We foresee three major aspects of the development of the proposed method: first, application of the method in a cardiac tissue engineering in order to control functional development of the tissue, second, development of the experimental tool allowing studying complex processes of propagation of excitation in a heart employing tissue culture, third, use of the digitally controlled tissue as a computing processor in a way it was done for the Belousov–Zhabotinsky reaction [1, 3, 5], and in a lab-on-chip systems [12].

Photosensitization of cardiac tissue. As a sensitizing substance we use azobenzene trimethylammonium bromide (AzoTAB) [13]. The dark, thermally relaxed, or obtained by irradiation with blue light ($\lambda > 440\,$nm) *trans*-isomer of AzoTAB reversibly reduces the occurrence of spontaneous activity, as well as decreases the speed of propagating excitation waves, up to total their suppression. The excitation waves may reactivate after irradiation with near-UV light ($\lambda \approx 365\,$nm), which produces prevalence of *cis*-isomer of AzoTAB. AzoTAB-mediated sensitization allows, thus, controlling the excitation waves through the entire cardiomyocyte network either uniformly, or in a preferred spatial pattern.

By mixing light with two wavelengths it is possible to obtain dynamically stable mixture of two isomers, maintaining constant concentration of the inhibitor, namely *trans*-isomer of AzoTAB. Let us denote $E_{\rm b}$ – intensity of blue light (440 nm), $E_{\rm uv}$ – intensity of UV-light (365 nm), A_0 – the total concentration of AzoTAB in the solution, $A_{\rm t}$ – concentration of *trans*-isomer, k_1 – rate of $cis \to trans$ photoisomerisation, k_2 – rate of $trans \to cis$ photoisomerisation. The *trans*-isomer of AzoTAB is more stable and it prevails in dark conditions hence we will denote k_3 the rate of dark thermal $trans \to cis$ isomerisation, which is independent on light, neglecting thermal $cis \to trans$ isomerisation:

$$\frac{dA_{\rm t}}{dt} = k_1(A_0 - A_{\rm t})E_{\rm b} - k_2 A_{\rm t} E_{\rm uv} + k_3(A_0 - A_{\rm t}). \quad (1)$$

For the constant concentration of *trans*-isomer $dA_{\rm t}/dt = 0$ and

$$A_{\rm t} = A_0 \frac{k_1 E_{\rm b} + k_3}{k_1 E_{\rm b} + k_2 E_{\rm uv} + k_3}. \quad (2)$$

Thermal relaxation of *cis*-isomer of AzoTAB is relatively slow, with the characteristic time of tens of minutes [13],

1) e-mail: agladze@yahoo.com

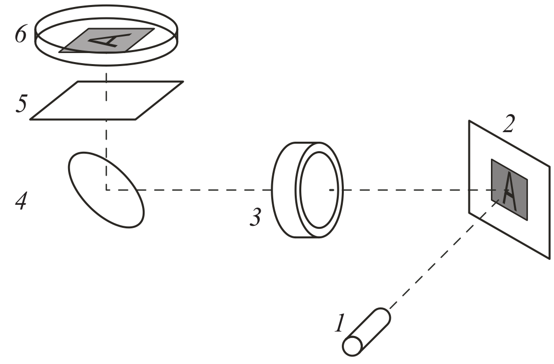

Fig. 1. A scheme of the setup: *1* – UV-diode, *2* – DMD-matrix of the projector, *3* – focusing lens, *4* – mirror, *5* – visible light cutting filter, *6* – petri dish with culture. The culture was observed from above

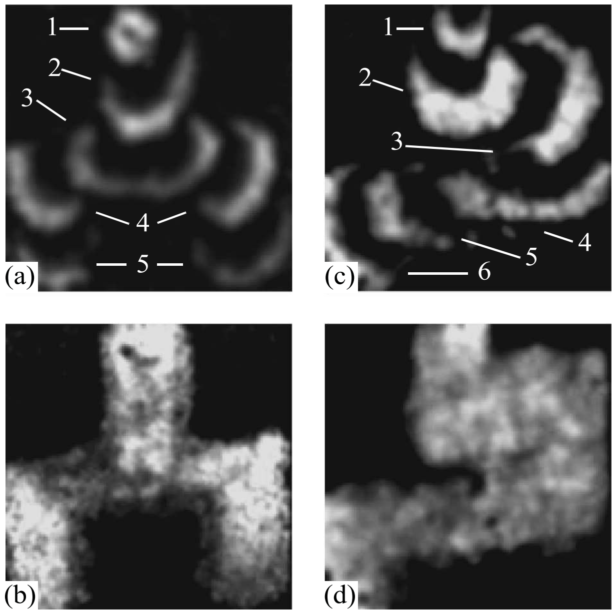

Fig. 2. Examples of projected pathways. (a), (c) – Sequences of the wave fronts. (b), (d) – Resulted pathways (projection of all fronts). The interval between consequent fronts is 0.32 s for frame (a) and 0.20 s for frame (c)

compare to the fast photoisomerisation which takes place within a few seconds for the illumination intensities of the order of $1\,\mathrm{mW/cm^2}$. Thus neglecting k3, we obtain

$$A_{\mathrm{t}} = A_0 \frac{n}{n+1}, \tag{3}$$

where $n = k_1 E_{\mathrm{b}}/(k_2 E_{\mathrm{uv}})$, and the concentration of *trans*-isomer of AzoTAB may be fine-tuned by changing the intensity ratio of UV and blue light. It is important to note that we always had a component of illumination with blue light since we used it for the fluorescence excitation while mapping the excitation pattern. However, when much greater intensity of UV-irradiation is applied, the concentration of *trans*-isomer of AzoTAB may be reduced to a negligible minimum.

2. Experimental setup. In order to perform photocontrol of the tissue layer we used modified digital projector Taxan KG-PL105S and coupled it with the macroview microscope Olympus MVX-10, Fig. 1. The spatial pattern of conducting pathways is created with the aid of computer graphic software and projected on the cardiomyocyte layer. Excitation waves were monitored using Ca^{2+}-sensitive fluorescent dye, Fluo-4 (Invitrogen) [14, 15]. Images were acquired using EM-CCD camera (iXon3, Andor) connected to a macro-view MVX10, Olympus microscope. The data were acquired at 50 frames per sec in 128×128 pixels resolution which correspond to $18 \times 18\,\mathrm{mm}^2$ area of the dish. The fluorescence of the dye was excited at $\lambda = 490\,\mathrm{nm}$ using the microscopeтАЩs light source unit outfitted with a mercury lamp and a blue bandpass filter. The same blue light source was used to induce *trans*-conformation of AzoTAB. To provoke the *trans*- to *cis*-transition we utilized the modified digital projector Taxan KG-PL105S equipped with 365 nm UV-LED module (LC-L2, Hamamatsu). The power densities of blue and UV lights at the culture were $3.5\,\mathrm{mW/cm^2}$ and $7.0\,\mathrm{mW/cm^2}$, respectively. The images were analyzed by image-processing system (ImageJ, NIH). To induce an excitation wave in some experiments we used electrical stimulation. The rectangular pulses with 1.5 to 4.0 V amplitudes and 20 ms duration were delivered via a 1 mm non-polarizing platinum electrode.

3. Results. 3.1 *Modeling different conducting pathways.* Our projection system allowed us to keep an intensity ratio between the UV-exposed and non-exposed

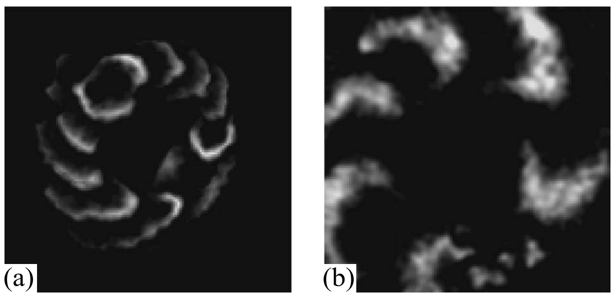

Fig. 3. Examples of the circular pathways. (a) – A sequence of fronts of the wave propagating in both directions of the circular pathway. The stimulating electrode induced the wave in the upper part of the pathway and wave pair annigilated in the bottom part. (b) – A sequence of fronts of the single wave propagating in circle. The interval between consequent fronts is 0.28 s for (a), and 0.30 s for (b)

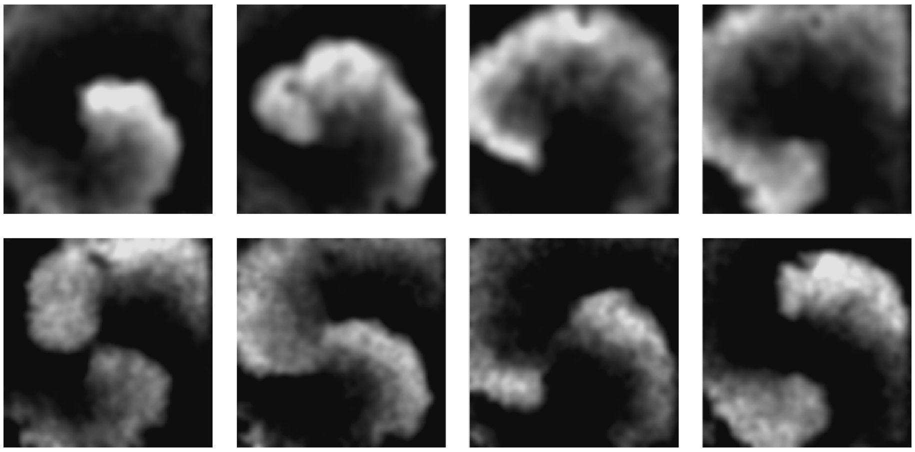

Fig. 4. Examples of the spiral waves obtained. Upper row: a snapshot sequence of the simple spiral or "re-entry". Lower row: a snapshot sequence of complex double spiral. The interval between consequent fronts is 0.40 s for the upper row and 0.30 s for the lower row

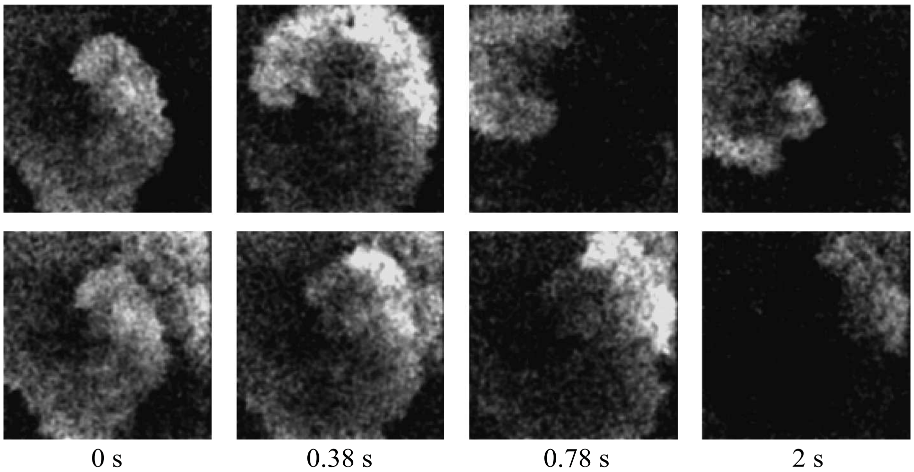

Fig. 5. A process of the spiral wave termination. Upper row: a snapshot sequence of the stable spiral wave. The interval between images is 0.5 s. Lower row: a snapshot sequence of the termination of spiral wave after decreasing the intensity of the UV by 40 %. The decreased intensity was still sufficient to provide wave propagation. Although it led to the spiral wave termination after about 5 min. The time passed since the first snapshot given under the frames

areas up to 10:1 which was sufficient for almost complete recovery of excitation in the UV-exposed area while keeping excitation totally suppressed in blue light – only exposed regions. Fig. 2 illustrates different pathways in the tissue culture created by projection of UV on the cardiomyocyte layer: Fig. 2a, b – Y shaped, or "fork", Fig. 2c, d – S shaped path. The edges of the pathways were slightly fuzzy with the characteristic transition between excitable and non-excitable area about 1 mm.

3.2 *Obtaining different types of "re-entry": propagation in a circle, spiral waves.* The photocontrolled cardiac tissue also allowed us to obtain rotating waves of excitation, as well as in the circular pathways (what cardiologists call "re-entry") and in the simply connected space – spiral waves. Fig. 3 shows wave propagation in a circular corridor, created by UV-projection. Fig. 3a illustrates annihilation of a symmetrically excited pair of excitation waves, while Fig. 3b shows circulation of the single wave. The latter case is due to non-symmetrical excitation (we stimulated culture to perform spiral wave, and then applied circular boundaries).

The spiral waves were initiated either by introducing by light a temporary inhomogeneity, or by application of fast pacing stimulation in the uniformly illuminated area. The examples of spiral waves obtained are shown in Fig. 4.

3.3. *Non-stationary regimes of propagation: perturbation of pinned spiral wave – termination.* Although, patterned excitable tissue may be created permanently by either patterned seeding of cells [13] or by partially removing them after attachment [15], it is much more challenging mission to produce excitable network with time-dependent parameters, relying on common tissue engineering methods. The digital photocontrol allows performing this task by simply changing light illumination intensity with time. We studied a process of perturbation of a stably rotating spiral wave by decreasing the excitability of the system with time. This procedure is directly related to the problem of termination of stable (functional) re-entry in the heart, as a common antiarrhythmic method [16, 17]. It is believed that stably rotating spiral waves in the cardiac tissue are so-called "pinned" waves, where heterogeneity in the core stabilizes the spiral wave [14], while unpinned, freely rotating waves are either intrinsically unstable or may migrate or drift in the naturally inhomogeneous cardiac tissue [14]. Recently it was shown that destabilization and termination of pinned waves can be done by applying external stimulation, either high-rate pacing [15], or with precise delivery of the stimulating pulse [18]. Our data show that decrease of excitability in the tissue may result in destabilizing spiral wave as well, and easily leads to its termination. The process of destabilization and termination of the spiral wave is illustrated in Fig. 5.

4. Conclusion. In the present article we show the method to digitally control cardiac tissue culture in order to model various regimes of excitation propagation in the cardiac tissue. This method provides a powerful tool for studying the behavior of the rotating spiral waves, especially in non-stationary time-dependent conditions. We expect this publication to be the first in a series of studies devoted to uncovering the biophysical mechanisms of tachyarrhythmia and heart failure.

---

1. L. Kuhnert, K.I. Agladze, and V.I. Krinsky, Nature **337**, 244 (1989).
2. A. Adamatzky, B. D. L. Costello, and T. Asai, *Reaction-diffusion computers*, Elsevier, 2005.
3. K. Agladze, N. Magome, R. Alieva et al., Physica D **106**, 247 (1997).
4. K. Agladze, R.R. Aliev, T. Yamaguchi, and K. Yoshikawa, J. Phys. Chem. **100**, 13895 (1996).
5. O. Steinbock, A. Tóth, and K. Showalter, Science **267**, 868 (1995).
6. I. N. Motoike, K. Yoshikawa, Y. Iguchi, and S. Nakata, Phys. Rev. E: Stat. Nonlinear Soft Matter Phys. **63**, 036220 (2001).
7. I. N. Motoike and K. Yoshikawa, Chaos Solitons Fractals **17**, 455 (2003).
8. N. Rambidi, K. E. Shamayaev, and P. G. Yu, Phys. Lett. A **298**, 375 (2002).
9. N. Bursac, K. K. Parker, S. Iravanian, and L. Tung, Circ. Res. **91**, 45e (2002).
10. X. Zong, H. Bien, Ch.-Y. Chung et al., Biomaterials **26**, 5330 (2005).
11. Y. Orlova, N. Magome, L. Liu et al., Biomaterials **32**, 5615 (2011).
12. J. Park, I. Ch. Kim, J. Baek et al., Lab Chip **7**, 1367 (2007).
13. N. Magome and K. Agladze, Physica D **239**, 1560 (2010).
14. K. Agladze, M. W. Kay, V. Krinsky, and N. Sarvazyan, Am. J. Physiol-Heart C. **293**, 503 (2007).
15. A. Isomura, M. Hörning, K. Agladze, and K. Yoshikawa, Phys. Rev. E **78**, 1 (2008).
16. F. H. Fenton, S. Luther, E. M. Cherry et al., Circulation **120**, 467 (2009).
17. S. Luther, F. H. Fenton, B. G. Kornreich et al., Nature **475**, 235 (2011).
18. M. Hörning, A. Isomura, K. Agladze, and K. Yoshikawa, Phys. Rev. E **79**, 026218 (2009).